Journal of
Instrumentation

OPEN ACCESS

Timing characterisation of TelePix2

To cite this article: H. Augustin *et al* 2025 *JINST* **20** C06071

Published by IOP Publishing for Sissa Medialab

Received: *February 7, 2025*
Accepted: *May 8, 2025*
Published: *June 27, 2025*

11th International Workshop
on Semiconductor Pixel Detectors for Particles and Imaging
Strasbourg, France
18–22 November 2024

2025 JINST 20 C06071

Timing characterisation of TelePix2

H. Augustin,[a] **L. Dittmann**,[a] **L. Huth**,[b] **D.M. Immig**,[a] **R. Kolb**,[a] **I. Perić**,[c] **A. Schöning**,[a] **F. Sefkow**,[b] **M. Stanitzki**,[b] **B. Weinläder**[a] and **A. Wintle**[b,*]

[a] *Physikalisches Institut der Universität Heidelberg, INF 226, 69120 Heidelberg, Germany*
[b] *Deutsches Elektronen-Synchrotron DESY, Notkestr. 85, 22607 Hamburg, Germany*
[c] *Institut für Prozessdatenverarbeitung und Elektronik, KIT, Hermann-von-Helmholtz-Platz 1, 76344 Eggenstein Leopoldshafen, Germany*

E-mail: arianna.wintle@desy.de

Abstract: The DESY II Test Beam Facility offers electrons with a user-selectable energy from 1–6 GeV primarily for detector characterisation. TelePix2, an HV-CMOS sensor, is new user-infrastructure at the test beam facility used as a Region of Interest (ROI) trigger for efficient small prototype testing and a timing plane for ambiguity suppression.

Here, timing characterisation results of TelePix2 are presented. A time resolution of $\sigma = 3.75(1)$ ns was determined at an efficiency above 99% at a depletion voltage of -85 V. Further timing improvements $\mathcal{O}(0.1\text{ ns})$ were achieved through offline corrections for delays dependent on hit position and time-walk. A time resolution of $\sigma = 2.216(3)$ ns from the signal of TelePix2 that can be used as a trigger was determined.

Keywords: Solid state detectors; Timing detectors; Trigger detectors

*Corresponding author.

https://doi.org/10.1088/1748-0221/20/06/C06071

Contents

1 Introduction

Stringent requirements on the performance of detectors for future high-energy physics and nuclear physics experiments drive the need for test beams. At test beam facilities, the performance of such devices can be evaluated under conditions similar to those experienced during the final operation. The DESY II Test Beam Facility in Hamburg, Germany [1], provides electron beams between 1–6 GeV primarily used for detector and device characterisation.

To support this, the test beam facility provides user infrastructure. This includes high-precision tracking devices called telescopes, two of which are EUDET-type telescopes [2] with Mimosa26 sensors [3, 4]. Relative to the rate of incoming electrons, the readout of these telescopes is slow, resulting in multiple electron tracks per readout frame. This creates ambiguities in associating particle hits to tracks, which is impossible to solve without adding a timing plane to associate hits with specific triggers. Additionally, a size mismatch between the trigger of the telescope and the device under test leads to inefficient data taking. To overcome this, a configurable region of interest trigger is needed.

2 TelePix2

TelePix2 [5] is a High Voltage Monolithic Active Pixel Sensor (HV-MAPS) developed to serve as both a Region of Interest (ROI) trigger and timing plane and the successor of the smaller sensor TelePix [6]. It provides timing with a timestamp binning of 4 ns.

The sensor is produced in the 180 nm HV-CMOS process of TSI, and benefits from the developments of the MuPix and AtlasPix series [7, 8]. The pixel matrix of 120 columns by 400 rows and a pixel size of $165 \times 25\,\mu m^2$ leads to an active area of $19.8 \times 10\,mm^2$. This is comparable to the size of the Mimosa26 sensors.

The amplifier and discriminator are located within the active pixel. Hit data is processed in digital partner cells on the periphery. The readout is a data-driven column drain scheme running at 1.25 Gbit/s. The DAQ of TelePix2 is based on the HV-MAPS laboratory and test beam DAQ developed in Heidelberg [9] and is fully integrated with EUDAQ2 [10] and the AIDA-TLU [11].

TelePix2 has a fast single-ended output line called the fast hit-OR, which is a logical OR of all unmasked pixels. The fast hit-OR, in combination with the ability to mask individual pixels, enables TelePix2 to function as a region of interest trigger.

Further technical details about the sensor, its operation, results obtained by initial users and details on efficiency can be found in [5].

2025 JINST 20 C06071

3 Test Beam performance

Data was taken at the DESY II Test Beam Facility at an energy of 4 GeV with the Adenium telescope [12] in beam line 22. An AIDA-TLU was used to sample a scintillator trigger signal, which was also used as a timing reference. A schematic of the setup used for data collection can be found in figure 1. The analysis was conducted in the Corryvreckan framework [13]. The TelePix2 operation settings include a depletion voltage of -85 V applied to the pixel guard rings, a supply voltage of 2 V and a comparator threshold of 16 DAC units above the baseline corresponding to 110(5) mV. The efficiency at the settings used in this proceeding was determined to be above 99 % [5]. 42 of the pixels were masked to minimise noise, leading to negligible noise levels. The sensor was operated without any cooling.

Telescope data is synchronised via trigger ID. Since no additional timing plane was used, a filter on single-track events is applied. Only the timestamp of the earliest pixel within track-associated clusters on TelePix2 was compared to the trigger timestamps recorded by the TLU.

TelePix2 is synchronised via a clock and reset signal from the TLU. Likely due to the mismatch of the TelePix2 clock (125 MHz) and the clock found within the rest of the test beam system (40 MHz), small offsets occur in timestamps between different data collection runs. These offsets have been corrected to combine the runs to gain the statistics necessary for subsequent plots.

Differences in TLU and TelePix2 timestamps as a function of pixel address can be found in figure 2(a). Approximately 8000 tracks per pixel were used to calculate these mean differences. Sharp jumps visible in the row dependency are attributed to metal layer changes in the signal routing impacting capacitance. The signals from distant rows have a larger delay due to increasing routing line capacitance. The small column dependency can potentially be caused by power distribution.

The mean time difference depends on Time Over Threshold (ToT) as visible in figure 2(b). The exact reason for the small side peaks observed in figure 2(b) is under investigation. Their occurrence at approximately ± 25 ns indicates an issue in sampling a 40 MHz clock within the system.

The pixel timestamps have been corrected in two steps: first on a pixel-by-pixel basis to correct for position-dependent effects and second by Time over Threshold (ToT) to compensate for time walk. Time residual distributions before and after these corrections can be found in figure 3. These distributions also include a minor contribution from the timing uncertainty of the TLU and scintillator, which is less than 1 ns. Only the results of a single run are shown to remove the uncertainty for offset correction between runs.

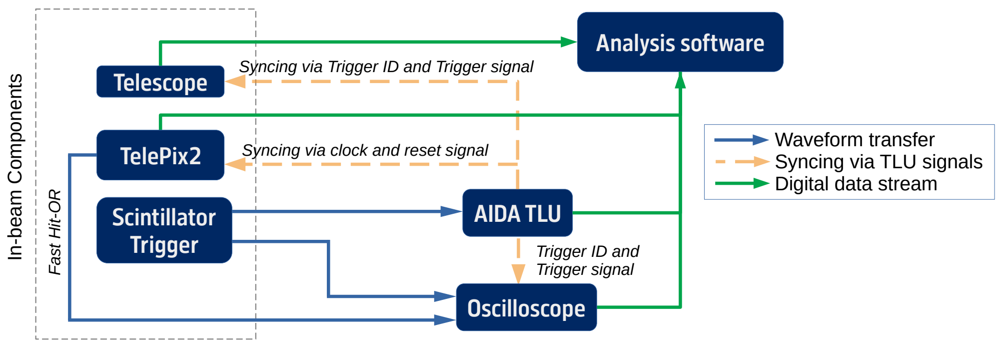

Figure 1. The test beam setup used for data collection. The AIDA TLU ensures the synchronisation of the telescope and TelePix2 with the trigger timestamps of the scintillator recorded by the TLU. Waveforms from the scintillator and TelePix2 fast hit-OR are saved alongside the trigger ID.

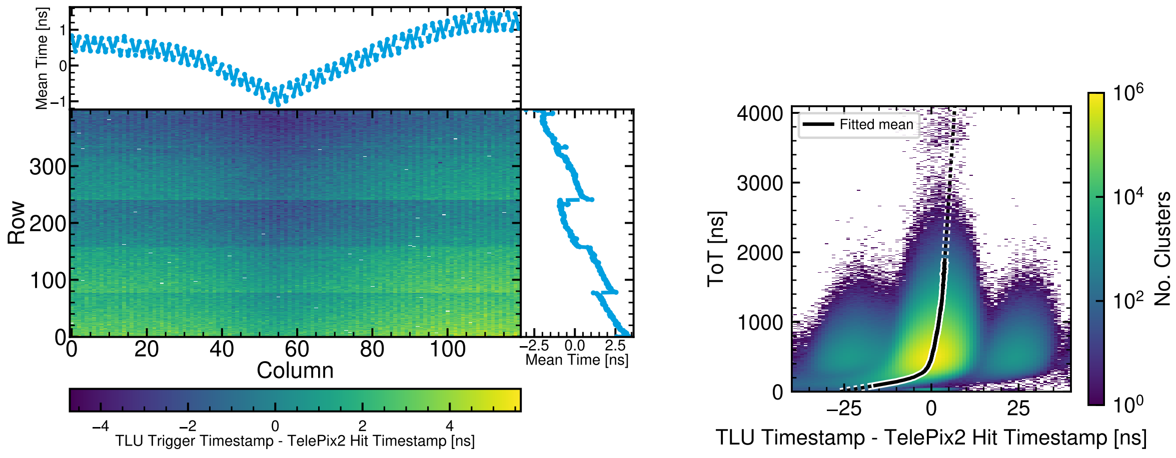

(a) (b)

Figure 2. Mean time difference between the timestamp of the scintillator trigger sampled by the TLU and the timestamp of the earliest hit within a cluster on TelePix2 as a function of pixel address (a) and Time over Threshold (ToT) (b). The mean time difference per pixel/ToT is extracted by a Gaussian fit of individual time residual distributions.

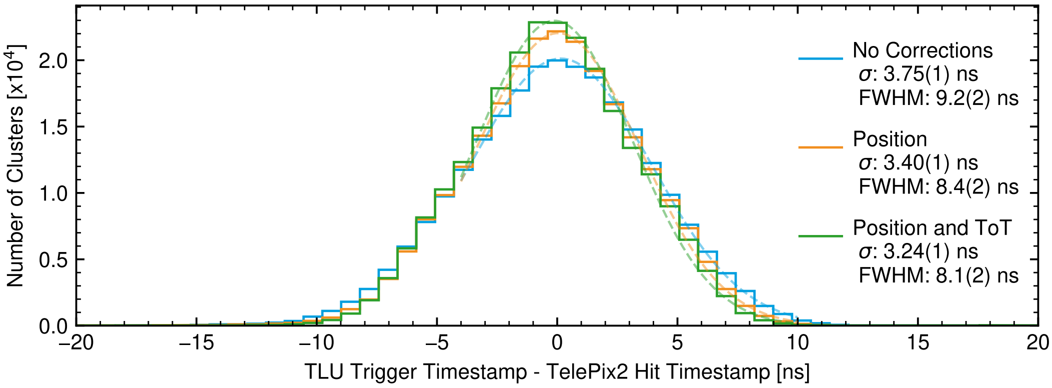

Figure 3. Timestamp time residuals before and after corrections.

Due to the non-Gaussian tails of the time residuals, timing performance was extracted in two ways: the sigma of a Gaussian fit of the core of the distribution (σ) and the full width at half maximum (FWHM). Before corrections, this leads to $\sigma = 3.75(1)$ ns and an FWHM of 9.2(2) ns. After position-based corrections, this reduces to $\sigma = 3.40(1)$ ns and an FWHM of 8.4(2) ns; further reducing to $\sigma = 3.24(1)$ ns and an FWHM of 8.1(2) ns after time walk corrections. Here, a clear improvement after correcting for position-based delays and time walk is shown.

The level of improvement gained by position-based corrections depends on the width of the incident beam. The more spatially homogenous the incident beam, the wider the range of position-based delays that influence the time residual distribution.

Waveforms of the fast hit-OR and a reference scintillator trigger signal were collected with an oscilloscope. The fast hit-OR is a pulse and contains no position information. To measure how the fast hit-OR timing performance varied across the sensor, the waveforms were matched on an event-by-event basis to TelePix2 clusters.

2025 JINST 20 C06071

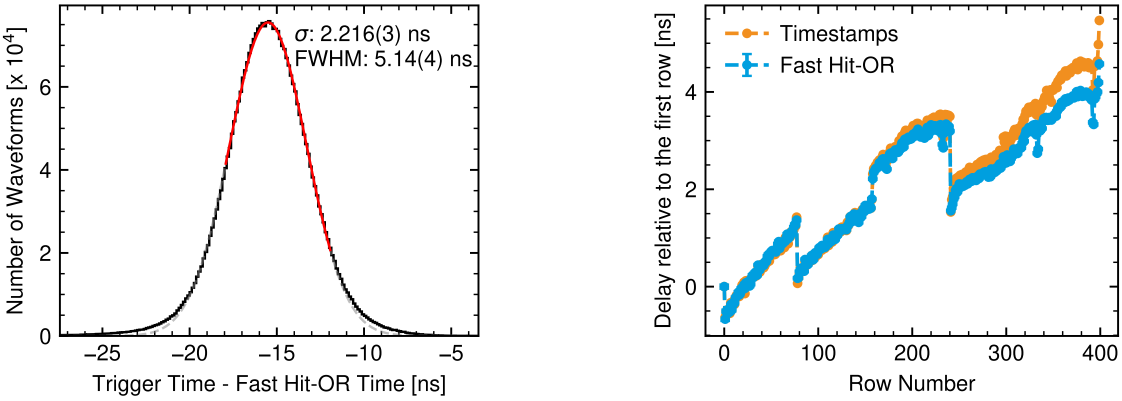

(a) (b)

Figure 4. Time difference between the scintillator waveforms and the fast hit-OR waveforms recorded by the oscilloscope, in agreement with [5] (a), and as a function of row with comparison to the row dependency of TelePix2 timestamps measured (b).

Timing of the fast hit-OR waveforms was extracted via threshold discrimination with a voltage of 0.4 V. This voltage was chosen due to the fast hit-OR's foreseen use case as a trigger signal.

As figure 4(b) shows, the fast hit-OR time delays with respect to row address exhibit a similar trend as those seen with the time stamps: sharp jumps due to the routing across different metal layers and an increase in delay with respect to increased distance from the periphery.

4 Conclusion

TelePix2 is the new timing plane and region of interest trigger for the DESY II Test Beam Facility. The two metrics were used to characterise the time residuals were the standard deviation of Gaussian fit to the core of the distribution (σ) and the full width at half max of the full distribution (FWHM). The TelePix2 timestamps showed a timing performance of σ = 3.75(1) ns and FWHM of 9.2(2) ns. The fast hit-OR, which can be used as a trigger signal showed a timing performance of σ = 2.216(3) ns with an FWHM of 5.14(4) ns. Offline timing corrections with respect to hit address and Time over Threshold (ToT) have shown improvements in timing O(0.1 ns).

Acknowledgments

The measurements leading to these results have been performed at the Test Beam Facility at DESY Hamburg (Germany), a member of the Helmholtz Association (HGF). This project has received funding from the European Union's Horizon 2020 Research and Innovation programme under GA no 101004761. We acknowledge support by the Deutsche Forschungsgemeinschaft (DFG, German Research Foundation) under Germany's Excellence Strategy – EXC 2121 "Quantum Universe" – 390833306.

References

[1] R. Diener et al., *The DESY II Test Beam Facility*, *Nucl. Instrum. Meth. A* **922** (2019) 265 [arXiv:1807.09328].

[2] H. Jansen et al., *Performance of the EUDET-type beam telescopes*, *EPJ Tech. Instrum.* **3** (2016) 7 [arXiv:1603.09669].

[3] J. Baudot et al., *First test results Of MIMOSA-26, a fast CMOS sensor with integrated zero suppression and digitized output*, in the proceedings of the *2009 IEEE Nuclear Science Symposium and Medical Imaging Conference*, Orlando, FL, U.S.A. (2009), p. 1169–1173 [DOI:10.1109/NSSMIC.2009.5402399].

[4] C. Hu-Guo et al., *First reticule size MAPS with digital output and integrated zero suppression for the EUDET-JRA1 beam telescope*, *Nucl. Instrum. Meth. A* **623** (2010) 480.

[5] L. Huth et al., *TelePix2: Full scale fast region of interest trigger and timing for the EUDET-style telescopes at the DESY II Test Beam Facility*, arXiv:2503.08177.

[6] H. Augustin et al., *TelePix — A fast region of interest trigger and timing layer for the EUDET Telescopes*, *Nucl. Instrum. Meth. A* **1048** (2023) 167947 [arXiv:2212.10248].

[7] I. Perić, *A novel monolithic pixelated particle detector implemented in high-voltage CMOS technology*, *Nucl. Instrum. Meth. A* **582** (2007) 876.

[8] R. Schimassek et al., *Test results of ATLASPIX3 — A reticle size HVCMOS pixel sensor designed for construction of multi chip modules*, *Nucl. Instrum. Meth. A* **986** (2021) 164812.

[9] H. Augustin et al., *The MuPix Telescope: A Thin, high Rate Tracking Telescope*, 2017 *JINST* **12** C01087 [arXiv:1611.03102].

[10] Y. Liu et al., *EUDAQ2 — A flexible data acquisition software framework for common test beams*, 2019 *JINST* **14** P10033 [arXiv:1907.10600].

[11] P. Baesso, D. Cussans and J. Goldstein, *The AIDA-2020 TLU: a flexible trigger logic unit for test beam facilities*, 2019 *JINST* **14** P09019 [arXiv:2005.00310].

[12] Y. Liu et al., *ADENIUM — A demonstrator for a next-generation beam telescope at DESY*, 2023 *JINST* **18** P06025 [arXiv:2301.05909].

[13] D. Dannheim et al., *Corryvreckan: A Modular 4D Track Reconstruction and Analysis Software for Test Beam Data*, 2021 *JINST* **16** P03008 [arXiv:2011.12730].

2025 JINST 20 C06071